CNRS
Centre National de la Recherche Scientifique

INFN
Instituto Nazionale di Fisica Nucleare

–Free Michelson calibration for Advanced Virgo– Constraints on minimum induced displacement of the mirrors and photodiode power estimations.

L. Rolland, R. Bonnand, R. Gouaty, F. Marion, B. Mours

VIR-0119A-13

April 10, 2013

VIRGO * A joint CNRS-INFN Project
Project office: Traversa H di via Macerata - I-56021 S. Stefano a Macerata, Cascina (PI)
Secretariat: Telephone (39) 50 752 521 – Fax (39) 50 752 550 – e-mail virgo@pisa.infn.it

Contents

1 Introduction **3**

2 Overview of the analytical calculations **3**

3 Overview of the simulation **5**

4 Comparison of calculation and simulation to VSR4 data **5**
4.1 Force and displacement applied to the mirrors during Virgo+ 6
4.2 Real data 7
4.3 Siesta simulations 10
4.4 Comparison 10

5 Simulation of AdV configurations **14**
5.1 Results 14

6 Conclusions **19**
6.1 Constraints on the mirror magnets and actuators 19
6.2 Constraints on the B1p longitudinal photodiode 19
6.3 Ideas of possible improvements 20

A ITF parameters used to estimate the DC and AC powers **22**

B Expected DC and AC powers in the different free Michelson configurations **24**

C Calculation of the demodulated power of the Michelson interferometer **28**

D Siesta configuration file of Virgo+ (WE-NI) **29**

E Siesta configuration file of AdV (WE-NI) **33**

F B1p readout **36**
F.1 B1p readout in Pr 36
F.2 History of B1p readout 37

1 Introduction

In order to calibrate the mirror actuators, the so-called *free swinging Michelson* technique was used during Virgo and will be used for AdV. This calibration method [1] is based on the non-linear reconstruction of the differential arm length (ΔL) of the Michelson interferometer from the continuous and the demodulated power at the antisymetric port (B1p beam). The reconstructed motion then allows to reconstruct the response of the actuator in m/V when some signal is sent to the electromagnetic actuators. During Virgo, this calibration was performed in the so-called high-power mode of the actuators, since a rather large motion of the mirrors was necessary to be able to measure it in the reconstructed channel.

In this note, two aspects of such data are studied:

- the calibration data sensitivity in ΔL is estimated: it puts constraints on the minimum displacement of the AdV mirrors to be induced by the electromagnetic actuators during calibration free swinging Michelson data (constraints for the PAY and SAT sub-systems).
- the continuous and demodulated powers sensed by the photodiode used on the B1p beam are estimated: it puts constraints on the readout electronics (constraints for the DET sub-system).

The beam powers are estimated from analytical calculations (section 2) and from time-domain simulations (section 3). The ΔL sensitivity is estimated running the non-linear reconstruction of the differential arm length on the simulated data.

First, in order to be confident in both the analytical calculations and the simulations, a first study has been performed using Virgo and Virgo+ configurations. The results have been compared to the data from VSR2 for Virgo and VSR4 for Virgo+. The comparisons are described in section 4.

Then the estimated DC and AC powers of the B1p beam and the noise level of the ΔL reconstructed channel have been simulated for AdV configurations in section 5.

Some ideas that could be further studied in the future to improve the calibration are given in section 6.3.

2 Overview of the analytical calculations

The Michelson ITF is described as in figure 1 with the following parameters:

- λ_0 and P_0, the input laser beam wavelength and power (ω_0 its pulsation),
- Ω and m the pulsation and depth of the frontal phase modulation of the input beam,
- the beam-splitter has amplitude reflection and transmission coefficients of $\sqrt{\frac{1}{2}}$,
- r_1 and r_2 are the amplitude reflection coefficients of the two arms,

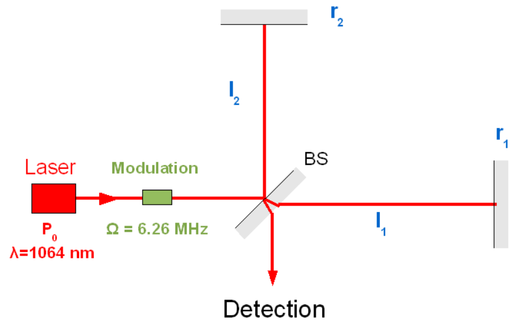

Figure 1: Simple Michelson configuration with frontal phase modulation.

- l_1 and l_2 are the lengths of the two arms.

Following appendix B of note [1], one can define:

$$J_0(m) \text{ and } J_1(m) \quad \text{the Bessel coefficients} \tag{1}$$

$$r = \frac{r_2 + r_1}{2} \quad \text{the average reflectivity} \tag{2}$$

$$\Delta r = \frac{r_2 - r_1}{2} \quad \text{the reflectivity asymmetry} \tag{3}$$

$$C = \frac{r^2 - \Delta r^2}{r^2 + \Delta r^2} \quad \text{the ITF contrast} \tag{4}$$

$$l_- = l_2 - l_1 \quad \text{the arm length difference} \tag{5}$$

$$T = \sin^2\left(\frac{\Omega}{c} l_-\right) \quad \text{the sideband transmission} \tag{6}$$

$$\Delta\Phi = 2\frac{\omega_0}{c} l_- \quad \text{the phase offset of the Michelson arms} \tag{7}$$

The analytical calculation has been first described in appendix B of note [1]. The formula for the DC power is correct, but some errors have been found in the AC power computation as summarized in appendix C.

The **continuous term** of the power transmitted by the ITF at the anti-symmetric port is:

$$P_{DC} = \beta\big(1 - \gamma\cos(\Delta\Phi)\big) \tag{8}$$

$$\text{with} \quad \beta = P_0\left(\frac{J_0^2}{2} + J_1^2\right)\left(r^2 + \Delta r^2\right) \tag{9}$$

$$\gamma = \left[1 - \frac{2J_1^2}{\frac{J_0^2}{2} + J_1^2} T\right] C \tag{10}$$

The **demodulated term** at Ω of the power transmitted by the ITF is:

$$P_{ACp} = \alpha_{ACp}\sin(\Delta\Phi) \tag{11}$$

$$\alpha_{ACp} = 2P_0 J_0 J_1 \sin\left(\frac{\Omega}{c} l_-\right)\left[r^2 - \Delta r^2\right] \tag{12}$$

3 Overview of the simulation

The time-domain simulation of the free swinging Michelson configurations have be performed using the Siesta software [2] (v5r02).

The **mirror suspensions** have been simulated using the *MIsa* card from Siesta, and the initial Virgo suspension descriptions provided in Siesta. They have not been adapated to AdV; in particular, the mass of the mirror has not been increased in the AdV simulations. The seismic noise have been included since it is one of the limiting noise in the reconstructed ΔL channel. The motions of the suspension along the beam (z) and around the x-axis[1] (θ_x) have been simulated since they are both strongly coupled to the longitudinal motion, while the other degrees of freedom have been frozen.

All the mirrors (PR, BS, NI, NE, WI, WE and SR) have been defined in the simulation, with their proper reflection and losses coefficients. The **optical simulation** has been performed using the *OPnode* card, such that the power lost by the misaligned mirrors in the real ITF is also lost in the simulation. A pick-off mirror has been simulated in order to extract a small fraction of the power at the anti-symmetric port, as done for the beam B1p in Virgo.

The **input laser beam** has been simulated with the carrier and two sidebands at the first modulation frequency (~ 6.26 MHz). The beam is described with the modal expansion method, including the TEM00, TEM01 and TEM10 modes (cards *IOlaser* and *OPmod*).

The **beam power detection** and demodulation has been done using the *OPdiode* card when no electronics noise was simulated and the *OPdet* card when adding electronics noise in the simulation. The powers given in this note are the power after the B1p pick-off (i.e. the power before any splitter is more than one photodiode is used to measure B1p).

The **simulated differential arm length** ΔL has been computed in Siesta from the positions of the different mirrors and saved in the simulated channels. It allows to compare the reconstructed ΔL to the initial one.

Examples of Siesta configuration files are given in appedix D for Virgo+ and E for AdV, both in the WE-NI Michelson configuration.

4 Comparison of calculation and simulation to VSR4 data

In this section, the calculations and simulations, performed with the ITF parameters as it was during the run VSR4 (June to September 2011), are compared to the real data. The real data are first described. Then the results of the simulations are given and conclusions are drawn.

4.1 Force and displacement applied to the mirrors during Virgo+

In Virgo+, the force applied to the mirror can be estimated from the signal sent to the actuation and the actuation response. The induced mirror displacement can then be estimated.

The calibration of the mirror actuators was done using free swinging Michelson data with the mirror actuation in high-power (HP) mode. In this mode, the calibration signal *zCorr* is converted into a current flowing in the coil through the DSP gains ($7.6 \times 1\,\mathrm{V/V}$), the DAC, and the trans-conductance amplifier with a gain of $0.15\,\mathrm{A/V}$. The geometry of the coil-magnet actuator is such that the conversion factor is estimated to[2] $2\,\mathrm{mN/A}$. As a consequence, the force per coil is estimated to $2.3\,\mathrm{mN/V}$.

For a sinusoidal force of amplitude ΔF and frequency f, the mirror motion Δx can then be estimated knowing the mass m (21.34 kg) of the mirror following the equation[3] (assuming two coils are used to move the mirror):

$$\Delta x(f) = -2 \times \frac{1}{m} \frac{\Delta F}{(2\pi f)^2} \qquad (13)$$

[1] The x-axis is the horizontal axis perpendicular to the beam axis.

[2] See VIR-NOT-ROM-1390-311 for initial magnets, and logbook entry 26630 for the values with magnets reduced by a factor ~ 5.

[3] This is true well above the mirror pendulum mechanical response frequency (0.6 Hz) and up to frequencies where internal mirror mode excitation cannot be neglected (few kHz when using the pairs of coil actuators on the side on the mirrors).

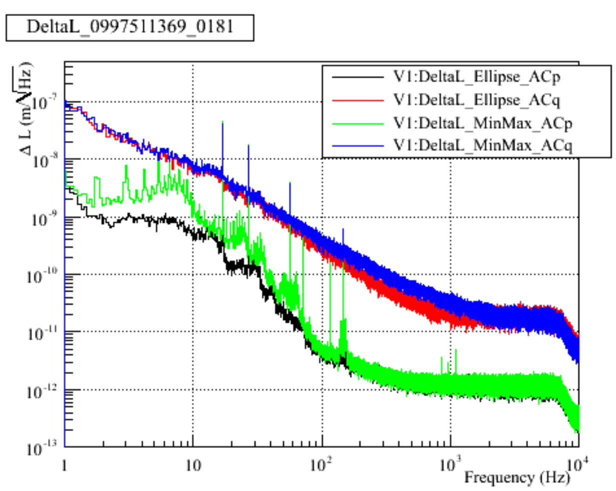

Figure 2: ***Reconstructed ΔL during WE-NI data during VSR4.*** *The lines at 71.5 Hz and 951.5 Hz were injected through the WE mirror, coils left-right, and the lines at 71.5 Hz, 116.5 Hz, 851.5 Hz and 951.5 Hz through the WE mirror, coils up-down, with zCorr amplitudes of ~ 0.19 V each. The lines at 17 Hz, 27 Hz, 57 Hz and 147 Hz were injected through the BS mirror. The line visible at 1111 Hz is a line used to control the laser frequency. Different signals and methods were used to reconstruct ΔL. The reconstruction used for the calibration is shown in black.*

For a 1 V amplitude excitation signal $zCorr$, the force amplitude is 4.6 mN and the mirror motion amplitude is 5.5×10^{-12} m at 1 kHz. It corresponds to the VSR4 measurements[4] shown in figure 2: a line at 951.5 Hz was injected through the WE mirror actuation with amplitude of 0.19 V during 180 s. It resulted in a reconstructed ΔL of $\sim 1 \times 10^{-12}$ m. Concerning the calibration, the coherence between the calibration signal $zCorr$ and the reconstructed ΔL was 0.74. The gain and phase were estimated to 18.3 ± 1.8 m/V and -9.7 ± 5.9 degrees respectively. The uncertainties are thus of the order of 10% and 100 mrad.
Note that such injections were done with amplitudes of the order of 1.4 V for each line at the input of the coil driver DAC, hence 2.8 V at the input of the DAC of WE actuation.

4.2 Real data

The raw signals extracted from the B1p photodiodes d1 and d2 are shown in figure 3 (during VSR4 data in WE-NI Michelson configuration). At that time, the DC and AC power signals were extracted from the photodiodes d1 and d2 respectively.

The spectrum of the reconstructed arm differential length ΔL is shown in figure 4(a) for data in WE-NI and in NE-WI Michelson configurations.

The shape of the B1p beam was monitored by a camera. The image of the beam is shown in figure 4(b). At first order, the beam looks gaussian, indicating that the Michelson mirrors were not too misaligned during the data taking.

Remarks on the calibration of the B1p photodiodes – The calibration coefficients used online for the B1p signals are given in appendix F for the runs VSR2, VSR3 and VSR4. The gains to convert the voltage in power are defined by resistances in the readout electronics, as well as by the gain of the demodulation electronics for the AC signals. The processed channels Pr_B1p_DC, ACp, ACq are the power of the B1p beam, before the splitter between the two photodiodes[5].

The online gains (in W/V) of the DC channels correspond within $\sim$ 20% to the expected values from the resistances used to readout the photodiode signal. The conversions of both channels $Pr\_B1p\_d1\_DC$ and $Pr\_B1p\_d2\_DC$ to a power using the DC gains are also in agreement within $\sim$ 20%. The offsets of the DC channels were not checked in this study, but there values are reasonable. This gives confidence in the absolute calibration of the B1p DC channels within $\sim$ 20%.

Concerning the AC channels of the B1p photodiodes, the voltage offsets can be estimated from the raw signals of the figure 3, in V, since the AC powers are expected to be symmetric around 0. The voltage offset can be converted in an offset in adc counts from the gain in V/adc

[4]see for example the VSR4 data at GPS 997511369 (August 16 2011).

[5] even before the pick-off mirror that pick 10% of the light towards the phase camera since mid-May 2009, see logbook entry 22904.

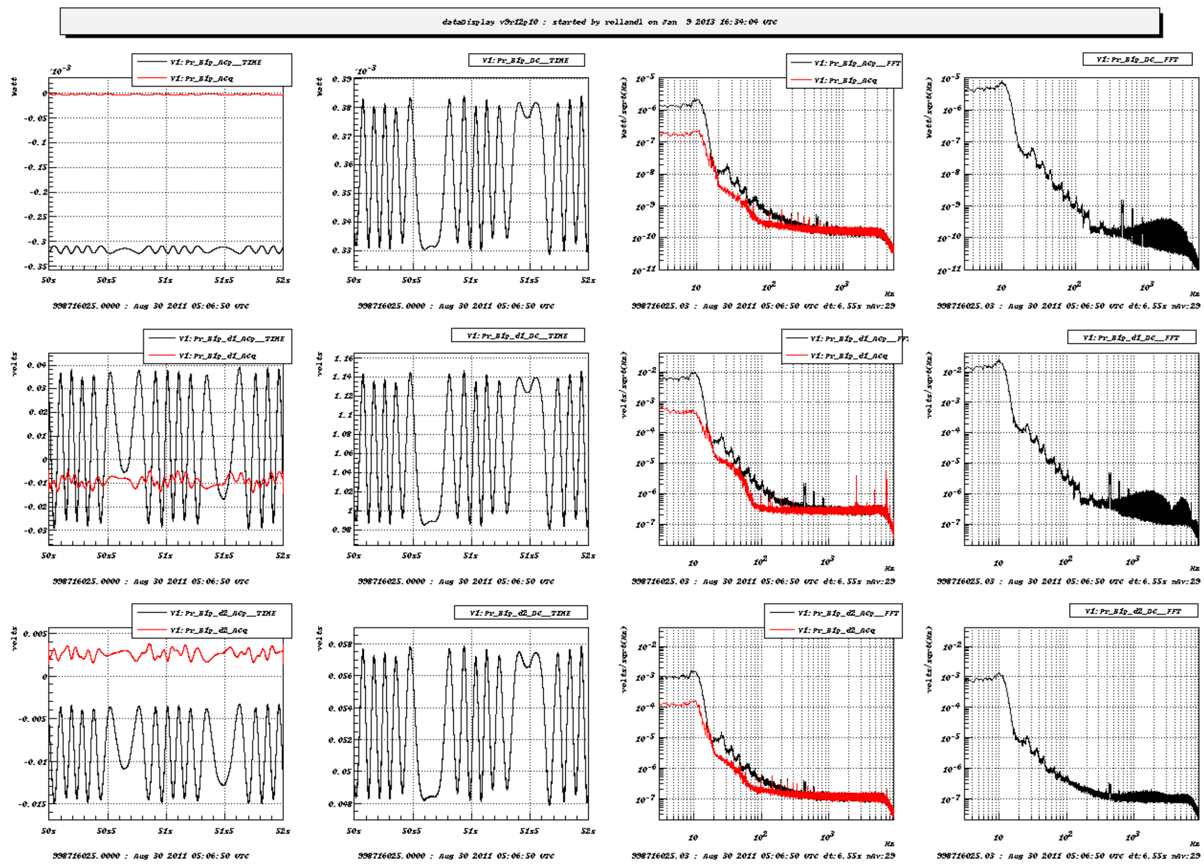

Figure 3: ***VSR4 WE-NI data: time series and spectrum of the B1p raw signals measured by the photodiodes*** *(GPS 998716025). First line: Pr_B1p (W). Second line: Pr_B1p_d1 (V). Third line: Pr_B1p_d2 (V). Times-series of AC (1st column) and DC (2nd column) signals over 2 s. Spectrum of AC (3rd column) and DC (4th column) signals (FFTs of 6.5 s, over 100 s). ACp in black and ACq in red. (a forest of lines at multiple of 10 Hz is visible at high frequency, mainly in the d1 DC channel)*

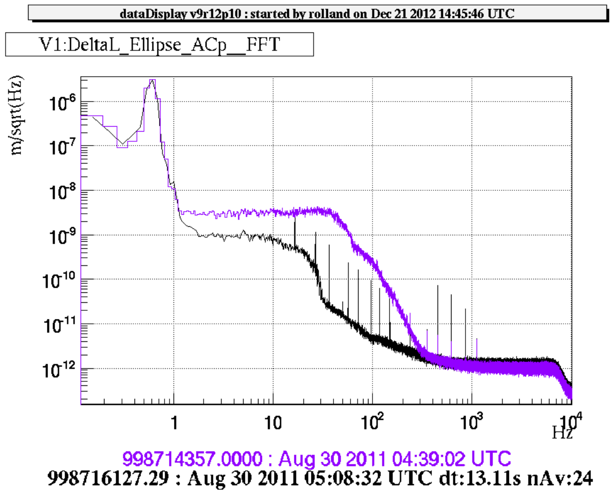

(a) Spectrum of the reconstructed ΔL.

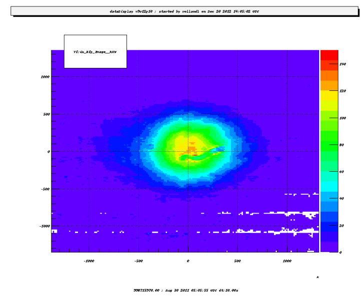

(b) Image of the B1p beam.

Figure 4: ***VSR4 WE-NI data****. (a) Black: WE-NI configuration. Purple: NE-WI configuration.*

count given in the appendix. It can then be compared to the offset used online and also given in the appendix.

During VSR3, the offsets values used online were reasonable, the larger difference being 366 adc counts (3.5 mV) on $B1p\_d1\_ACq$. During VSR4, the offsets values used online are much more different than expected for the ACp channnels with offsets of the order of 135000 and 24000 adc counts (or 1.30 V and 0.230 V) for the d1 and d2 channels respectively (both correspond to $\sim 155\,\mu$W offset).

Assuming that the offsets might not be well defined, the AC gains (W/V) can be checked looking at the peak-to-peak values of the AC channels. It has been checked that the d1 and d2 AC gains are compatible together, giving the same peak-to-peak power within better than a factor 2.

As a conclusion, both d1 and d2 channels of B1p have compatible DC calibration within 20% and the absolute values can be trusted. The gains of the AC channels are also compatible within a factor 2 between d1 and d2 photodiodes, but the offsets are not properly set. As a consequence, the peak-to-peak values of Pr_B1p_ACp, ACq might be trusted within a factor 2, but not the absolute values.

High-frequency noise floor – In Virgo+, in the asymmetric Michelson configurations, the DC power of B1p was of the order of $P_{DC} \sim 0.350\,$mW. It results in a shot noise of $\sqrt{2h\nu P_{DC}} \sim 1.1 \times 10^{-11}$ W. As shown in figure 5(a), the noise floor of the power spectrum is ten times higher. It indicates that it is limited by the electronics noise.

4.3 Siesta simulations

As described in section 3, simulations of the Virgo+ interferometer have been performed to reproduce the WE-NI Michelson configuration.

The AC and DC powers of the simulated B1p signal are shown as times-series and spectrum in figure 5(a). After data processing, the spectrum of the reconstructed ΔL is shown in figure 5(b).

Impact of electronic noise – From both the data and the simulation, the shot noise is found to be of the order of 10^{-11} W and the electronics noise is limiting the sensitivity to $\sim 10^{-10}$ W above ~ 100 Hz. Different noise levels have been modified in the simulations in order to show their effects on the sensitivity in term of ΔL.
In case of a factor 10 more noise in the AC channels only, no additionnal noise is visible in the DC channel, the noise of the demodulated power increases by $\sim \sqrt{10}$, and the noise floor of the ΔL spectrum increases by less than a factor 2.
In case of a factor 10 more noise in the DC channel only, the noise is directly visible in the DC channel, the noise of the demodulated power increases by $\sim \sqrt{10}$, and the noise floor of the ΔL spectrum increases by a factor 10.

Non-linear noise – As shown in figure 5(b), the bump around 20 Hz visible in the ΔL spectrum is not present if only the TEM00 mode of the laser beam is simulated. It must be due to non-linear coupling of the low frequency seismic noise to the longitudinal motion, probably through the θ_x degree of freedom of the mirrors.
"Arches" are visibles in the spectrum as function of time of the data and of the simulations as shown in figure 6. The coupling will be studied later and is not described in this note.

Other remarks – In the intermediate frequency range, the noise floor of the NE-WI configuration is lower than in the WE-NI configuration.. This is due to the fact that the transmission factor of the sideband is lower in the WE-NI configuration ($T = 0.76$) than in the NE-WI configuration ($T = 0.92$). However, it is the opposite in the VSR4 data as shown in figure 4(b), and with a larger difference. The reason is not understood. It could be due to a stronger non-linear noise coupling in the NE-WI data, but the reason is not known yet.

4.4 Comparison

Powers – The table 1 summarizes the powers of the B1p beam simulated with siesta, computed analytically, and measured in the WE-NI and NE-WI Michelson configurations during Virgo (VSR1, in 2007) and Virgo+ (VSR4, in 2011).

The simulation and the analytical computation are in agreement for the DC and AC powers.

The estimations are over-estimated by a factor of ~ 1.4 compared to the VSR1 data. Taking into account this factor, the agreement is within better than 10%.

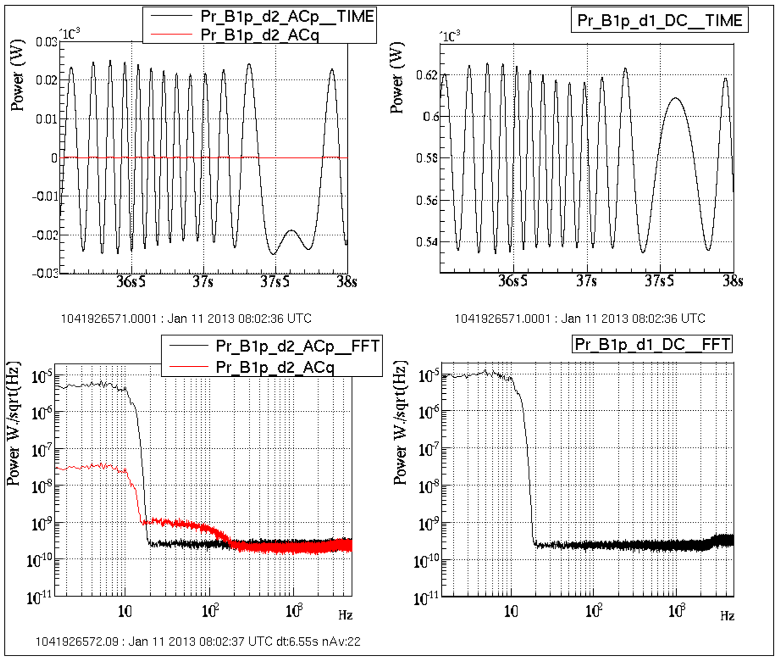

(a) Simulated time-series and spectrum of photodiode signals (WE-NI).

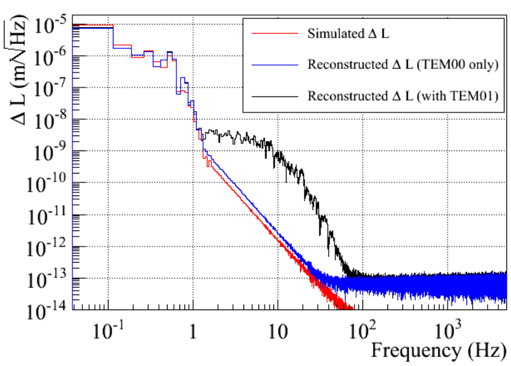

(b) Simulated spectrum of ΔL (WE-NI).

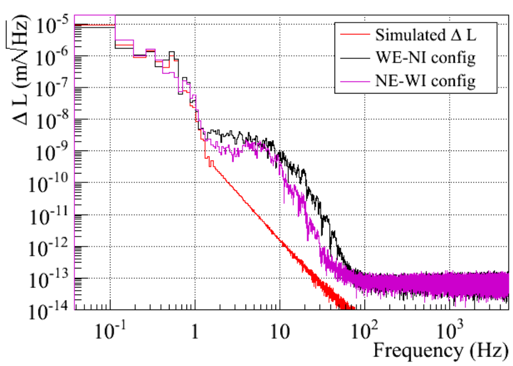

(c) Simulated spectrum of ΔL.

Figure 5: ***Simulated Virgo+ configurations.*** *(a) WE-NI configuration. All y-axis units are watts. First line: times-series of AC and DC signals over 2 s. Second line: spectrum of AC and DC signals (FFTs of 6.5 s). ACp in black and ACq in red. (b) Reconstructed ΔL in WE-NI configuration. Red: simulated ΔL. Black: reconstructed ΔL with the standard simulation. Blue: reconstructed ΔL when only the TEM00 mode of the laser is simulated. (c) Comparison of reconstructed ΔL in WE-NI (black) and NE-WI (purple) configurations (red: simulated ΔL).*

			Simulation	Analytical	Data	Data/Theory
VSR1	WE-NI	$< DC >$ (mW)	0.280	0.281	0.206	0.73
		ΔDC (mW)	0.127	0.129	0.093	0.73
		ΔAC (mW)	0.073	0.065	0.043	0.66
	NE-WI	$< DC >$ (mW)	–	0.281	0.207	0.73
		ΔDC (mW)	–	0.129	0.095	0.73
		ΔAC (mW)	–	0.073	0.047	0.64
	NI-WI	$< DC >$ (mW)	0.553	0.554	0.400	0.72
		ΔDC (mW)	1.11	1.11	0.800	0.73
		ΔAC (mW)	0.069	0.069	0.048	0.70
VSR4	WE-NI	$< DC >$ (mW)	0.520	0.522	0.357	0.68
		ΔDC (mW)	0.080	0.082	0.059	0.72
		ΔAC (mW)	0.045	0.042	0.017	0.40
	NE-WI	$< DC >$ (mW)	0.520	0.522	0.355	0.68
		ΔDC (mW)	0.080	0.081	0.060	0.74
		ΔAC (mW)	0.045	0.046	0.020	0.43

Table 1: Comparison of simulation and data (WE-NI configuration during VSR4). The average DC power is given, as well as the peak-to-peak (Δ) of the DC and AC powers. See tables 5 and 6 for more details and GPS times of the data.

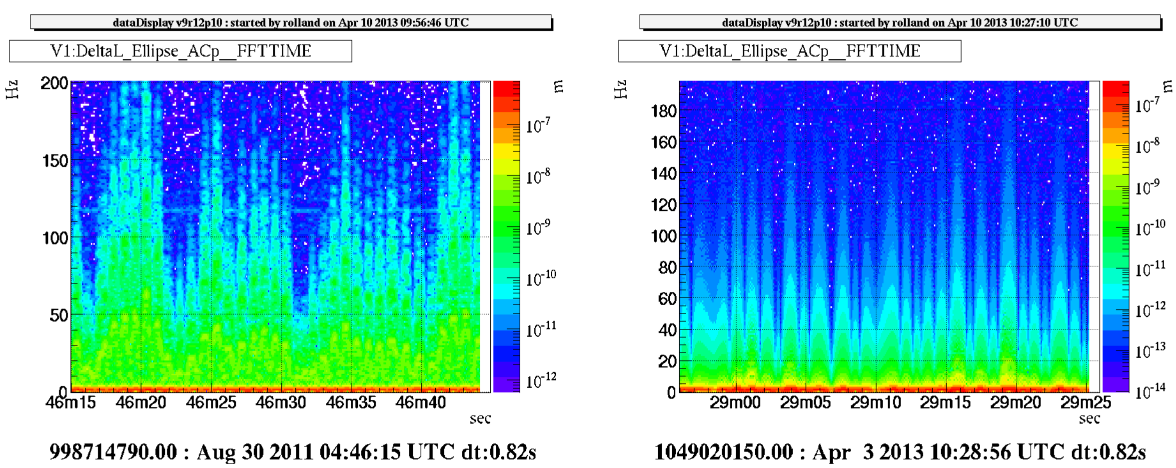

(a) Data

(b) Simulation.

Figure 6: ***FFT of*** ΔL_{rec} ***vs time*** *for data and simulated data.*

Compared to VSR4 data, the estimations are also over-estimated, by factors ~ 1.4 and ~ 2.5 for the DC and AC powers respectively. The DC has still the same difference than during VSR1, while the AC powers have larger different. This difference is not unexpected since the B1p photodiode calibration must have been less precise after different modifications (see section 4.2 on p. 9 and appendix F).

The spectrum of the DC and AC power channels are given in figures 3 and 5(a) for the VSR4 data and the VSR4 simulation respectively. The behavior of simulation is similar to the one of the data.

A plateau is visible below 10 Hz, with measured values of $5 \times 10^{-6} W/\sqrt{Hz}$ in DC and $2 \times 10^{-6} W/\sqrt{Hz}$ in AC, the simulated plateau being a factor ~ 2 lower.

The high frequency noise is also at similar levels within 50%, with measured values of $1 \times 10^{-10} W/\sqrt{Hz}$ in DC and $2 \times 10^{-10} W/\sqrt{Hz}$ in AC.

In the mid-frequencies, between 10 Hz and a few hundred's hertz, the noise measured in the data is not reproduced in the siesta simulations.

Reconstructed ΔL – The spectrum of the reconstructed ΔL are given in figures 4(a) and 5(b) for the VSR4 data and the VSR4 simulation respectively. The behavior of the simulation is also similar to the one of the data. A plateau is visible in the range 1–10 Hz, with noise level of $10^{-9}\,\mathrm{m}/\sqrt{\mathrm{Hz}}$ in the data and a factor 2 higher in the simulation. At high frequency, the noise floor is limited at $10^{-12}\,\mathrm{m}/\sqrt{\mathrm{Hz}}$ in both cases. In the mid-frequencies, the noise structure is also more complicated in the data than in the simulations.

Conclusions – As a conclusion, the siesta simulation reproduces the general behaviour of the data taken in free swinging Michelson configurations during Virgo+. The B1p powers are understood within a factor ~ 2.

5 Simulation of AdV configurations

In the previous section, it has been shown that the siesta simulations reproduce the general behaviour of the free swinging Michelson data in term of photodiode power and noise, and in term of noise of the reconstructed differential arm length ΔL. Such simulations have thus been done for the different AdV configurations: power recycled ITF with input beam of 25 W (PR_25W), dual recycled ITF with input beam of 25 W (SR_25W), and dual recycled ITF with input beam of 125 W (SR_125W). The mirror positions, reflectivities and losses have been extracted from the AdV Technical Design Report [3]. The B1p photodiode is assumed to receive 0.3% of the output beam.

The electronics of the photodiode readout of AdV is not yet finalized. However, the noise of the AdV readout electronic of the photodiode is expected to be equivalent to a shot-noise[6] of the order of 10^{-10} W. The simulations shown in this section are done **without electronics noise**. The shot-noise limited high frequency noise floor has to be extrapolated: the ΔL noise floor is proportionnal to the (equivalent) shot noise.

The suspensions have not been updated in the simulation: the configurations are still the ones from Virgo. In particular, the mass of the mirrors was not increased by a factor 2.

No specific signal has been sent to the mirror actuators to simulate the calibration signals.

As a consequence, the results of the simulation are expected to give the behavior of the B1p DC and AC powers, as well as the noise level of the reconstructed ΔL channel when it is shot-noise limited.

5.1 Results

The time-series and spectrum of the simulated shot-noise limited DC and AC powers as well as the spectrum of the reconstructed ΔL are shown in figures 7, 8 and 9 for the PR_25W, SR_25W and SR_125W respectively.

The table 2 summarizes the DC and AC powers of the B1p beam, assuming that the pick-off represents 0.3% of the output beam (B1) power[7]. The shot-noise is also given, as well as the high frequency noise floor of the reconstructed ΔL signal. The expected noise floor assuming the readout electronics noise is equivalent to a shot-noise of 10^{-10} W is indicated in the table and in the ΔL spectrum.

As in Virgo, the dynamic of the power signals is of 5 orders of magnitude when shot-noise limited. The configuration SR_25W is the less sensitive in term of reconstructed ΔL, with

[6] In Science Mode, the electronics noise for AdV readout electronics is expected to be a factor ~ 2 below the shot noise, and the power on the nominal photodiodes is ~ 50 mW. As a consequence, the shot noise is 1.4×10^{-10} W and the electronics noise should be below 10^{-10} W.

[7] and a single photodiode for B1p.

a shot noise limited floor of $8 \times 10^{-12}\,\mathrm{m}/\sqrt{\mathrm{Hz}}$. Assuming the readout electronics has a noise equivalent to a shot-noise of $10^{-10}\,W$, **the noise floor is increased to** $1 \times 10^{-11}\,\mathrm{m}/\sqrt{\mathrm{Hz}}$.

Config	Parameter	PR_25W	SR_25W	SR_125W
WE-NI	$< B1p\_DC >$ (mW)	0.822	0.164	0.822
	$\Delta B1p\_DC$ (mW)	0.045	0.0091	0.045
	$\Delta B1p\_AC$ (mW)	0.009	0.0018	0.009
	Shot noise level (W)	2×10^{-11}	8×10^{-12}	2×10^{-11}
	Shot-noise limited ΔL floor ($\mathrm{m}/\sqrt{\mathrm{Hz}}$)	3×10^{-13}	8×10^{-13}	3×10^{-13}
	Expected ΔL floor ($\mathrm{m}/\sqrt{\mathrm{Hz}}$)	1.5×10^{-12}	1×10^{-11}	1.5×10^{-12}

Table 2: Summary of AdV powers of the B1p beam, shot-noise limited noise-floor of the reconstructed ΔL and expected noise-floor including electronics noise in different Michelson configurations.

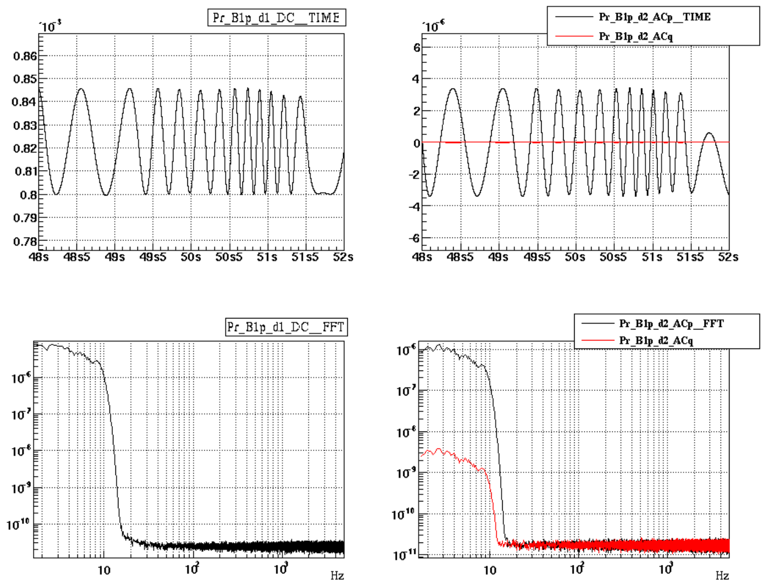

(a) AdV, PR, 25W: simulated B1p power time-series and spectrum (W).

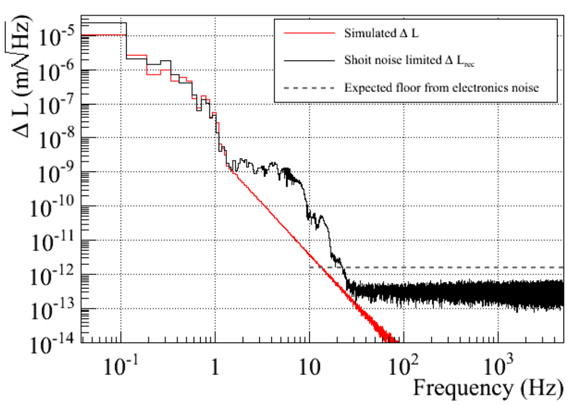

(b) AdV, PR, 25W: simulated spectrum of reconstructed ΔL.

Figure 7: ***Simulated time series and spectrum of the B1p power signals and reconstructed*** *ΔL for th AdV, PR_25W WE-NI configuration. (a) All y-axis units are watts. First line: times-series of AC and DC signals over 2 s. Second line: spectrum of AC and DC signals (FFTs of 6.5 s). ACp in black and ACq in red. (b) Simulated ΔL in red, reconstructed shot-noise limited ΔL in black. Dotted line: expected floor from B1p electronics noise.*

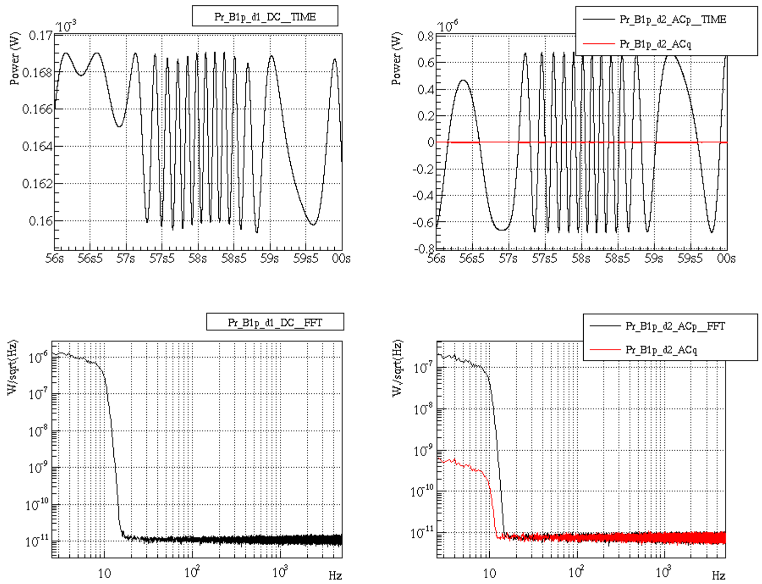

(a) AdV, SR, 25W: simulated B1p power time-series and spectrum (W).

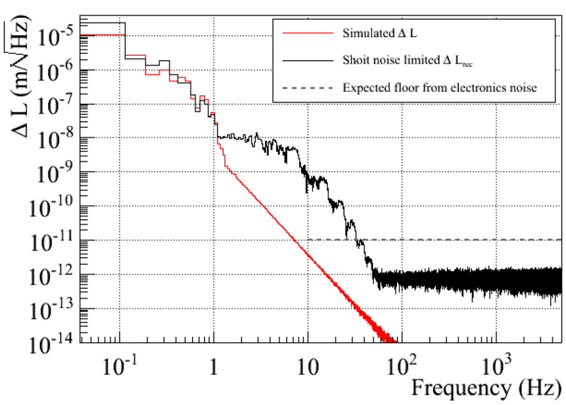

(b) AdV, SR, 25W: simulated spectrum of reconstructed ΔL.

Figure 8: ***Simulated time series and spectrum of the B1p power signals and reconstructed*** *ΔL for the AdV, SR_25W WE-NI configuration. (a) All y-axis units are watts. First line: times-series of AC and DC signals over 2 s. Second line: spectrum of AC and DC signals (FFTs of 6.5 s). ACp in black and ACq in red. (b) Simulated ΔL in red, reconstructed shot-noise limited ΔL in black. Dotted line: expected floor from B1p electronics noise.*

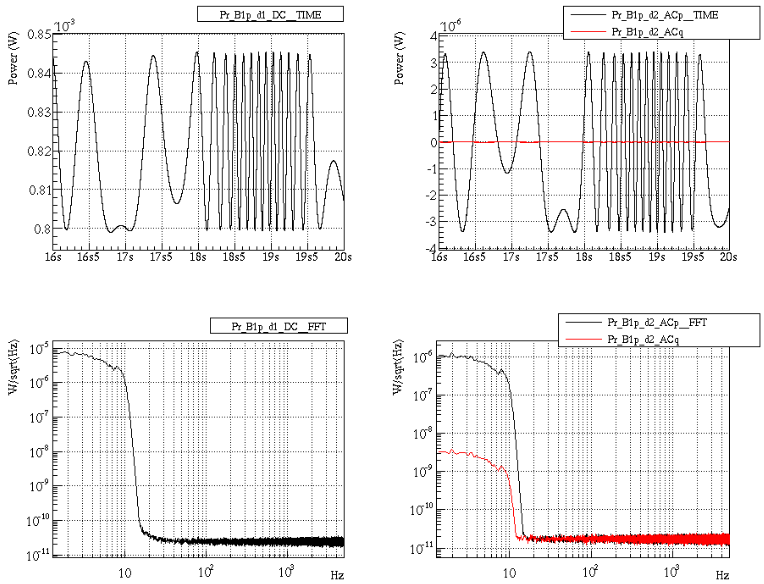

(a) AdV, SR, 125W: simulated B1p power time-series and spectrum (W).

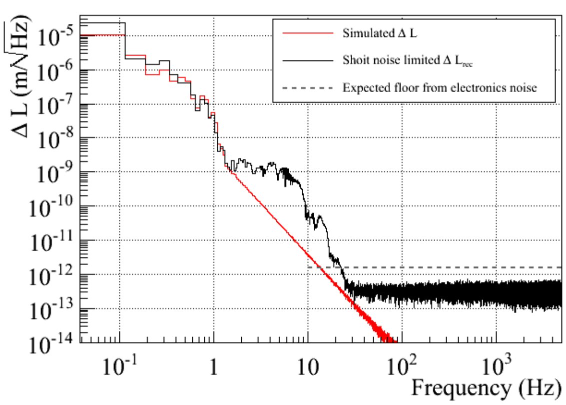

(b) AdV, SR, 125W: simulated spectrum of reconstructed ΔL.

Figure 9: ***Simulated time series and spectrum of the B1p power signals and reconstructed*** *ΔL for the AdV, SR_125W WE-NI configuration. (a) All y-axis units are watts. First line: times-series of AC and DC signals over 2 s. Second line: spectrum of AC and DC signals (FFTs of 6.5 s). ACp in black and ACq in red. (b) Simulated ΔL in red, reconstructed shot-noise limited ΔL in black. Dotted line: expected floor from B1p electronics noise.*

6 Conclusions

The analytical calculations of the B1p DCand AC powers as well as the time-domain simulations of the free swinging Michelson data have been validated though comparisons with Virgo andn Virgo+ data.

They have then been used to simulate AdV configurations. The time-domain simulations have shown that it will be possible to calibrate the AdV mirror actuators using the free swinging Michelson technique as during Virgo. However, constraints are drawn in order to be able to inject sine signals up to ∼1 kHz to the mirrors such that the induced motion is visible in the reconstructed ΔL.

6.1 Constraints on the mirror magnets and actuators

As a consequence for PAY and SAT sub-systems, one should be able to induce mirror motion of the order of a few 10^{-11} m at 1 kHz (in HP mode), when taking free swinging Michelson data, on the NE, WE, NI, WI and BS mirrors. This constraint is driven by the SR, 25 W configuration of AdV. It could be relaxed when the laser power will be increased (towards 10^{-12} m at 1 kHz in HP mode in SR, 125 W configuration.

In order to translate the mirror actuation calibration parameters from HP mode to LN_i modes, additional constraints also apply on the coil driver electronics: it is mandatory to have a coil current sensing channels that is used to monitor the current in at least two consecutive modes with exactly the same sensing electronics (i.e in at least HP and LN1 mode, and at least LN_i and LN_{i+1} modes).
Note that the main part of the actuation calibration systematic uncertainties during Virgo came from this so-called *HP to LN calibration*. It is thus also recommanded to have the possibility to measure the current in the coils through a second sensing electronics in order to cross-check the measurements and study systematic effects.

6.2 Constraints on the B1p longitudinal photodiode

The expected noise of the AdV photodiode readout electronics is equivalent to a shot noise a bit lower than 10^{-10} W (see section 4.3). This level of noise would limit the ΔL sensitivity above a few 10's of Hz.

In order to be shot-noise limited, the B1p electronics noise should be lower than the shot-noise expected for a DC power of ~ 1 mW, i.e. an equivalent shot-noise of 10^{-11} W. This must not be achievable, but the gain of the B1p photodiode channel might be adapted to reduce the noise towards this value.

6.3 Ideas of possible improvements

The following ideas could help to improve the sensitivity of the free Michelson ΔL measurements, and hence the actuator calibration precision. Not all are easily feasible.

- better tune the demodulation phase than during Virgo.

- better understand and try to subtract the non-linear coupling of the low frequency seismic noise into the band 1 Hz to 100 Hz.

- use other sidebands than 6.27 MHz (i.e. 8.36 MHz, 56 MHz or 131 MHz) to increase the sideband transmission T (see equation 6). The average DC power is independent of T and the DC power variations are very low dependence on T. So changing the sideband used in the analysis would not modify the shot noise level. However, the AC power variations are proportional to $\sqrt{T}$. The sideband transmission T are shown in table 3 for the different modulation frequencies and the different Michelson configurations. The 6.27 MHz sideband is the best in the asymetric configurations, so no improvements can be done compared to what was shown in this note. In the short Michelson configuration, the 121 MHz sideband could be used, but it might have a lower modulation index which might compensate the effect. The 56 MHz sideband might be the best one in the short Michelson configuration.

- lock the OMCs in order to use the B1 beam which is ~ 300 times more powerful. The lock of the OMCs when the beam is flashing due to the fringes of the Michelson configuration must be a difficult task. This solution cannot be taken for granted.

- modify (increase) the laser power and/or the modulation depth when taking FM data. It must not be possible to modify these parameters by large amounts. An increase of laser power of 20% would improve the ΔL sensitivity by $\sim 9\%$. An increase of the modulation depth by a factor 2 would improve the ΔL sensitivity by ~ 2.

- increase the B1p pick-off power during calibration data. This would need to have the B1p pickoff optics on motorized mounts: it is not planned nor easily feasible.

Frequency (MHz)	6.270777	56.436993	8.361036	131.686317
NI-WI	0.0011	0.0020	**0.088**	**0.42**
WE-NI	**0.997**	0.69	0.79	0.21
WE-NI	**0.999**	0.77	0.98	0.91

Table 3: Transmission (T) of the different sidebands in the different Michelson configurations.

References

[1] L. Rolland, F. Marion, B. Mours, *Mirror motion reconstruction for free swinging Michelson data* (2008) VIR-112A-08.

[2] B. Caron et al, *SIESTA, a time domain, general purpose simulation program for the VIRGO experiment* (1999) Astroparticle Physics **10** 4, pp. 369-386

[3] The Virgo collaboration, *Advanced Virgo Technical Design Report* (2012) VIR-0128A-12TDR.

[4] P. Puppo and P. Rapagnani, *The Electromagnetic Actuators of the Mirror Reaction Masses* (2005) VIR-NOT-ROM-1390-311.

[5] E. Tournefier et al., *Upgrade of the detection bench electronics* (2004) VIR-NOT-LAP-1390-270.

A ITF parameters used to estimate the DC and AC powers

The table 4 summarizes the parameters used in the analytical calculation and SIESTA simulations. The Virgo+ configuration corresponds to Virgo+ with the monolithic suspensions installed.

Laser powers of VSR1 and VSR4 have been estimated from the channel Sc_IB_TraMC: it is the power transmitted by the input mode-cleaner, that reaches the PR mirror.

The parameter $R_{B1p}^{transparent}$ is a coefficient factor to pick-off the B1p beam that is corrected, in the data in the data acquisition (PrITF.cfg file), or also in the calculation and simulations. As a consequence, the given powers are the power of B1p before the splitter than separate the beam towards the two photodiodes.

Configuration		Virgo (VSR1)	Virgo+ (VSR4)	Advanced Virgo PR, 25W	Advanced Virgo SR, 25W	Advanced Virgo SR, 125W
Laser	P_0 (W)	8	14	25	25	125
	$\frac{\Omega}{2\pi}$ (MHz)	6.2642	6.2642	6.270777	6.270777	6.270777
	m	0.28	0.28	0.1	0.1	0.1
BS	R_{BS}	0.5	0.5	0.5		
	L_{BS}	0	0	0		
WE	L_2 (m)	3000.0812	3000.0812	2999.80		
	R_{WE}	0.999962	0.999989	0.999999		
	L_{WE}	0	0	0		
NE	L_1 (m)	3000.0812	3000.0812	2999.80		
	R_{NE}	0.999962	0.999989	0.999999		
	L_{NE}	0	0	0		
WI	l_2 (m)	5.634	5.634	5.786		
	R_{WI}	0.883	0.9586385	0.986		
	L_{WI}	308 ppm	308 ppm	204 ppm		
NI	l_1 (m)	6.512	6.512	6.041		
	R_{NI}	0.882	0.9587387	0.986		
	L_{NI}	325 ppm	325 ppm	204 ppm		
PR	R_{PR}	0.9487	0.9487	0.95		
	L_{PR}	0	0	530 ppm		
SR	R_{SR}	–	–	0	0.80	0.80
	L_{SR}	–	–	230 ppm	130 ppm	130 ppm
B1p pickoff	$R_{B1p}^{pickoff}$	0.0034	0.0034	0.0030		
	$R_{B1p}^{transparent}$	0.5	0.90×0.5	0.0030		
	ϵ	0.90	0.90	0.90		

Table 4: Parameters used in the Siesta simulations for the different ITF configurations. For AdV, losses of NI and WI include the compensating plates and losses of PR include the pick-off plate. For AdV, l1 and l2 take into account the mirrors and CP widths (with material index of 1.45) $l1 = 0.065\sqrt{2}\times 1.45 + 5.367 + 0.035\times 1.45 + 0.200 + 0.200\times 1.45$. $l2 = 5.245 + 0.035\times 1.45 + 0.200 + 0.200\times 1.45$..

B Expected DC and AC powers in the different free Michelson configurations

The equations are taken from appendix B of note [1]. The ITF parameters in the different configurations are the one described in appendix A The code to make the calculations can be found in the Cali package v0r3p16, in the script file FreeMichelson.C, function $FM\_TheoreticalSignals$.

For Virgo, the analytical calculation and the SIESTA simulations are in agreement (see tables 5 and 6).

The 7 first lines of the tables give values of parameters defined in section 2. The average value of the DC power and the peak-to-peak (Δ) values of the DC and AC powers are then given: P^{out} is the power after the BS mirror ; P^{B1p} is the power of the B1p beam pick-off (as if only one photodiode to measure it).

For AdV, the analytical calculation and the SIESTA simulations are in agreement concerning the DC powers, while there is a 30% difference in the AC power. This difference has not been understood yet, but it does not have strong impact on the results of this note.

	Parameter	WI-NI	WE-NI	NE-WI
Calculation	T	0.0132	0.761	0.924
	C	1	0.244	0.247
	α/P_{BS}	0.0276	-0.0259	-0.0289
	β/P_{BS}	0.441	0.224	0.224
	α (W)	0.0113	-0.0106	-0.0119
	β (W)	0.181	0.0918	0.092
	γ	0.999	0.23	0.229
	ΔP_{DC}^{out} (mW)	362	42.2	42.1
	ΔP_{AC}^{out} (mW)	22.6	21.3	23.7
	$< P_{DC}^{B1p} >$ (mW)	0.554	0.281	0.281
	ΔP_{DC}^{B1p} (mW)	1.11	0.129	0.129
	ΔP_{AC}^{B1p} (mW)	0.069	0.065	0.073
Simulation	$< P_{DC}^{B1p} >$ (mW)	0.553	0.280	
	ΔP_{DC}^{B1p} (mW)	1.11	0.127	
	ΔP_{AC}^{B1p} (mW)	0.0693	0.073	
VSR1 data	$< P_{DC}^{B1p} >$ (mW)	0.400	0.206	0.207
	ΔP_{DC}^{B1p} (mW)	0.800	0.093	0.095
	ΔP_{AC}^{B1p} (mW)	0.048	0.043	0.047

Table 5: **Virgo (VSR1).** *Last 3 lines are VSR1 measurements from GPS 875298420 (NI-WI), 866373720 (WE-NI) and 866375440 (NE-WI). They are in agreement with the data shown in figure 2 of note [1] (October 2007). Note that the demodulation phase was not adjusted for the AC channels, and that ACq was used for NE-WI data while ACp was used for NI-WI data.*

	Parameter	WI-NI	WE-NI	NE-WI
Calculation	T	0.0132	0.761	0.924
	C	1	0.0837	0.0835
	α/P_{BS}	0.03	-0.00953	-0.0105
	β/P_{BS}	0.479	0.24	0.24
	α (W)	0.0215	-0.00684	-0.00752
	β (W)	0.344	0.172	0.172
	γ	0.999	0.0788	0.0776
	ΔP_{DC}^{out} (mW)	687	27.2	26.7
	ΔP_{AC}^{out} (mW)	43	13.7	15
	$< P_{DC}^{B1p} >$ (mW)	1.04	0.522	0.522
	ΔP_{DC}^{B1p} (mW)	2.08	0.082	0.081
	ΔP_{AC}^{B1p} (mW)	0.13	0.042	0.046
Simulation	$< P_{DC}^{B1p} >$ (mW)	–	0.520	0.520
	ΔP_{DC}^{B1p} (mW)	–	0.080	0.080
	ΔP_{AC}^{B1p} (mW)	–	0.044	0.044
VSR4 data	$< P_{DC}^{B1p} >$ (mW)	–	0.357	0.360
	ΔP_{DC}^{B1p} (mW)	–	0.059	0.070
	ΔP_{AC}^{B1p} (mW)	–	0.017	0.025

Table 6: **Virgo+ with monolithic suspensions.** *Last 3 lines are measurements obtained during VSR4, at GPS 998715966 for WE-NI and 998714196 for NE-WI. The demodulation phase was roughly adjusted so that the ACp channel contains most of the signal.*

	Parameter	WI-NI	WE-NI	NE-WI
Calculation	T	0.00112	0.997	1
	C	1	0.0278	0.0278
	α/P_{BS}	0.00329	-0.00136	-0.00136
	β/P_{BS}	0.493	0.246	0.246
	α (W)	0.00407	-0.00169	-0.00169
	β (W)	0.609	0.305	0.305
	γ	1	0.0275	0.0275
	ΔP_{DC}^{out} (mW)	1.22e+03	16.8	16.8
	ΔP_{AC}^{out} (mW)	8.14	3.37	3.37
	$< P_{DC}^{B1p} >$ (mW)	1.65	0.823	0.823
	ΔP_{DC}^{B1p} (mW)	3.29	0.0453	0.0453
	ΔP_{AC}^{B1p} (mW)	0.022	0.0091	0.0091
Simulation	$< P_{DC}^{B1p} >$ (mW)	–	0.823	–
	ΔP_{DC}^{B1p} (mW)	–	0.045	–
	ΔP_{AC}^{B1p} (mW)	–	0.0068	–

Table 7: **AdV, PR, 25 W**

	Parameter	WI-NI	WE-NI	NE-WI
Calculation	T	0.00112	0.997	1
	C	1	0.0278	0.0278
	α/P_{BS}	0.00329	-0.00136	-0.00136
	β/P_{BS}	0.493	0.246	0.246
	α (W)	0.00407	-0.00169	-0.00169
	β (W)	0.609	0.305	0.305
	γ	1	0.0275	0.0275
	ΔP_{DC}^{out} (mW)	1.22e+03	16.8	16.8
	ΔP_{AC}^{out} (mW)	8.14	3.37	3.37
	$< P_{DC}^{B1p} >$ (mW)	0.329	0.164	0.164
	ΔP_{DC}^{B1p} (mW)	0.658	0.0091	0.0091
	ΔP_{AC}^{B1p} (mW)	0.00439	0.0018	0.0018
Simulation	$< P_{DC}^{B1p} >$ (mW)	–	0.164	–
	ΔP_{DC}^{B1p} (mW)	–	0.009	–
	ΔP_{AC}^{B1p} (mW)	–	0.0014	–

Table 8: **AdV, SR, 25 W**

	Parameter	WI-NI	WE-NI	NE-WI
Calculation	T	0.00112	0.997	1
	C	1	0.0278	0.0278
	α/P_{BS}	0.00329	-0.00136	-0.00136
	β/P_{BS}	0.493	0.246	0.246
	α (W)	0.0203	-0.00843	-0.00844
	β (W)	3.05	1.52	1.52
	γ	1	0.0275	0.0275
	ΔP_{DC}^{out} (mW)	6.09e+03	83.9	83.9
	ΔP_{AC}^{out} (mW)	40.7	16.9	16.9
	$< P_{DC}^{B1p} >$ (mW)	1.64	0.822	0.822
	ΔP_{DC}^{B1p} (mW)	3.29	0.045	0.045
	ΔP_{AC}^{B1p} (mW)	0.022	0.0091	0.0091
Simulation	$< P_{DC}^{B1p} >$ (mW)	–	0.822	–
	ΔP_{DC}^{B1p} (mW)	–	0.045	–
	ΔP_{AC}^{B1p} (mW)	–	0.068	–

Table 9: **AdV, SR, 125 W**

C Calculation of the demodulated power of the Michelson interferometer

The calculation is based on the description done in appendix B of note [1], with some corrections:

- equation 24 of [1]: a factor 2 is missing for the signals at Ω and 2Ω (in front of the real parts ($\Re$)). This factor 2 then has to be applied in all equations of section B.2.2.
- the factor 1/2 that appears when multiplying the two cosines is corrected in the Virgo demodulation electronics. So another factor 2 has to be applied to the equations on p.30 of [1].
- the main error is the statement in p.30 of [1] that $rr_{sb} - \Delta r \Delta r_{sb} \sim rr_{sb}$: this is true in the case of a symmetric Michelson (short or long Michelson configurations), but both terms are of similar amplitudes in the case of non-symmetric Michelson as the WE-NI and NE-WI configurations mainly used for the mirror actuator calibration.

Finally, assuming the demodulation phase is tuned to have $P_{ACq} = 0$ and all the signal in P_{ACp}, one has to rewrite equations 34–36 from [1]:

$$P_{ACp} = \alpha_{ACp} \sin(\Delta\Phi) \quad (14)$$

$$\alpha_{ACp} = 2P_0 J_0 J_1 \sin(\frac{\Omega}{c} l_-) \left[r^2 - \Delta r^2\right] \quad (15)$$

D Siesta configuration file of Virgo+ (WE-NI)

```
/* $Id: freeMich_WENI_OPnode_VirgoP.car,v 1.1 2012/12/11 16:49:15 rolland Exp $ */

/* Simulate 130 s for suspension "warm-up" and 70 s of data usable for reconstruction */
/* maximum clock rate for OPglobal : 100 kHz */
UJclock masterClocks 4000000 4   20000. 10000. 1000.  1.

/*UFrBuilder name clock firstrun firstframe triggerType */
UFrBuilder FBuilder 3 1 1  1

/* Seismic noise */
/* Noise motion description: clock   amplitude   F_lowpass  correlation_distance*/
GRound 2    5e-7  0.6  0.

/* Noise motion at one point */
GRoundPt Mbs  0.     0.     0.
GRoundPt Mwe  0.     3005.6 0.
GRoundPt Mni  5.8    0.     0.

/*Simulate an initial excitation of the mirrors: sine at 0.2 Hz with linear decrase of amplitude during 0.5 s */
  USignal BSexcFreq  0.317                                      /* Hz */
  USsweep BSexcAmplTmp 0  2e-6 -2e-6                            /* Linear variation */
  USline  BSexcTmp     0  BSexcAmplTmp.out BSexcFreq 0.0        /* Generate sine signal with decreasing amplitude */
  USif    BSexc        0  BSexcAmplTmp.out > 0 BSexcTmp.out NULL   /* Use sine signal only when amplitude is positive */
/* Force to be applied on BS mirror.  2.2V on zCorr, with 1.1 mN/V/coil -> 2.4 mN applied on each magnet */
UScosine       BSline1   0   2.2          37.0      0
UScosine       BSline2   0   2.2         117.0      0
UScosine       BSline3   0   2.2         237.0      0
USadder zBS 0 4 BSline1.out BSline2.out BSline3.out  BSexc.out
/*              0.0825       0.0825       0.0825        0.0  */
/*                 0            0            0            1.0  */
                   0            0            0            0.0

/* Simulation of actuation  */
/*MIact name clock input f_AA(Hz) nBits DACmax(V) DACnoise(V/rHz)  gain Vmax  Imax    Rcoil  Fcoil  alpha(N/A) */
/* Since in HP mode, there is a transconductance ampli, the gain is 0.15 A/V, so we assumed Rcoil=1 and Fcoil is very high,
   being the cut-off frequency of the amplifier */
MIact   fBS 0 zBS.out    3e3      20    10.       2.5e-6          0.15 20.   1.0     1      9e3   10.6e-3


/*  USignal WEexcFreq  0.695                                    */  /* Hz */
/*  USsweep WEexcAmplTmp 0  1e-5 -1e-5                          */  /* Linear variation */
/*  USline  WEexcTmp     0  WEexcAmplTmp.out WEexcFreq 0.0      */ /* Generate sine signal with decreasing amplitude */
/*  USif    WEexc        0  WEexcAmplTmp.out > 0 WEexcTmp.out NULL */ /* Use sine signal only when amplitude is positive */
/* Force to be applied on WE mirror. 0.2 V on zCorr, with 2.2 mN/V/coil -> 0.44 mN applied on each magnet */
UScosine       WEline1   0   0.2         451.5     0
UScosine       WEline2   0   0.2         616.5     0
UScosine       WEline3   0   0.2         851.5     0
USadder zWE_UD 0 3 WEline1.out WEline2.out WEline3.out  /* WEexc.out  */
/*                 7.6          7.6          7.6 */         /* 0.0        */
                   0            0            0
MIact   fWE_UD 0 zWE_UD.out   3e3   20   10.   2.5e-6    0.15    20.  1.0   1   9e3   1.9e-3

UScosine       WEline4   0   0.3          36.5     0  /* 0.31 V  *2.2 mN/V/coil */
UScosine       WEline5   0   0.2        1036.5     0  /* 0.22 V  *2.2 mN/V/coil */
USadder zWE_LR 0 2 WEline4.out WEline5.out
/*                 7.6          7.6          */
                   0            0
MIact   fWE_LR 0 zWE_LR.out   3e3   20   10.   2.5e-6    0.15    20.  1.0   1   9e3   1.9e-3


/* ************************************************************************ */
/* --------------- Definition of the suspension and mirrors ----------------*/
/* ************************************************************************ */

/* ******* PR ****** */
MIrror   MirPR 1 NULL NULL MiSuPRf NULL -6.085 0. 0. 1. 0. 0.
MIsurf   MiSuPRf 6.99154e-4     .2  0.  0.  0.   0.9487     0e-6

/* ******* BS ****** */
/*
Thermal     ThBS  1 5  28  15     4e6   16e6    36e6
                       0.6 4.7e3  300   600     900
                       1e6 1e6    1e5   1e5     1e5
*/
MIsa SuBS 1 Mbs.dxyzt    "/users/rolland/home/myDev/Cali/v0r3p16/siesta/bs_tuned.sad"
                         4
                         ref_1 fBS.out
                         ref_2 fBS.out
                         ref_3 fBS.out
                         ref_4 fBS.out
```

```
                         0
                         "freeze(x,y,ty,tz)"
                        /* "defaults" */
/* Definition of the mirror */
/* MIrror name clock suspPos thermPos   fSurf bSurf  x y z tx ty tz */
MIrror   MirBS 0 SuBS.dxyzt NULL MiSuBSf MiSuBSb 0.0  0.0  0.0 -0.7 0.7 0.
/* Misurf name 1/curvature radius thetax thetay halfthickness reflection losses (in intensity) */
MIsurf   MiSuBSf 0.        .2     0.     0.     0.0       0.50      0.0e-6
MIsurf   MiSuBSb 0.        .2     0.     0.     0.0       0.00      0.0e-6

/* ******* WE ****** */
/*
Thermal  ThWE 1 1 28
                  0.5955
                  1.e6
*/
MIsa SuWE 1 Mwe.dxyzt    "/users/rolland/home/myDev/Cali/v0r3p16/siesta/Tower6000.sad"
                         4
                         ref_1 fWE_LR.out  /* Coil R */
                         ref_2 fWE_LR.out  /* Coil L */
                         ref_3 fWE_UD.out  /* Coil U */
                         ref_4 fWE_UD.out  /* Coil D */
                         0
                         "freeze(x,y,ty,tz)"

MIrror      MirWE 1 SuWE.dxyzt  NULL MiSuWEf NULL   0. 3005.7152 0.   0. -1. 0.
MIsurf      MiSuWEf  2.80112e-4 .2 0.  0.  0.   0.999989 0

/* ******* NI ****** */
/*
Thermal  ThNI 1 1 28
                  0.5955
                  1.e6
*/
MIsa SuNI 1 Mni.dxyzt    "/users/rolland/home/myDev/Cali/v0r3p16/siesta/Tower6000.sad"
                         0
                         0
                         "freeze(x,y,ty,tz)"

MIrror   MirNI 1 SuNI.dxyzt  NULL MiSuNIf MiSuNIb   6.512 0. 0.   1. 0. 0.
MIsurf   MiSuNIf  0.            .2  0.  0.  0.   0.9587387  0
MIsurf   MiSuNIb  0.            .2  0.  0.  0.   0.          325e-6

/* ******* NE ****** */
MIrror      MirNE 1 NULL  NULL MiSuWEf NULL   3006.5932 0.  0.   -1. 0. 0.
MIsurf      MiSuNEf  2.80112e-4  .2  0.  0.  0.   0.999989    0

/* ******* WI ******** */
MIrror   MirWI 1 NULL  NULL MiSuWIf MiSuWIb   0. 5.634 0.    0. 1. 0.
MIsurf   MiSuWIf  0.            .2  0.  0.  0.   0.9586385  0
MIsurf   MiSuWIb  0.            .2  0.  0.  0.   0.          308e-6

/* ********************************************************************** */
/* --------------------------- Laser simulation -----------------------------*/
/* ********************************************************************** */

/*Input laser beam */
/* IOlaser  name clock surface lambda   power powerNoise     freqNoise curvature       waist   window grid order */
IOlaser    laser 0      NULL    1064e-9 14.  NULL           NULL       0.        0.049060     0.     NO
1

/*Modulation: OPmod name clock input nfreq  list_of_freq  signals_for_amplitude_modulation */
/* Initial beam approximation */
OPmod    mod   0  laser.oBeam  3  0. 6.2642e6 -6.2642e6 carrier NULL sb1 NULL sb2 NULL
USignal carrier  0.9804958   /* Bessel J0 factor for modulation depth of 0.28 */
USignal sb1      0.1386325   /* Bessel J1 factor for modulation depth of 0.28 */
USignal sb2     -0.1386325

/* ********************************************************************** */
/* ----------------------- Light propagation ---------------------------*/
/* ********************************************************************** */

/* PR transmission of INJ beam */
OPnode nodePRf 0      mod.oBeam        NULL   MiSuPRf
/* BS front */
OPnode nodeBSf_in  0  nodePRf.tBeam     NULL   MiSuBSf

/* W arm: WI input */
OPnode nodeWIb_in  0  nodeBSf_in.rBeam  NULL   MiSuWIb
OPnode nodeWIf_in  0  nodeWIb_in.tBeam  NULL   MiSuWIf
/* W arm: WE */
OPnode nodeWEf     0  nodeWIf_in.tBeam  NULL   MiSuWEf
/* W arm: WI output */
OPnode nodeWIf_out 0  nodeWEf.rBeam     NULL   MiSuWIf
```

```
OPnode nodeWIb_out 0  nodeWIf_out.tBeam NULL   MiSuWIb

/* N arm: BS back */
OPnode nodeBSb_in  0  nodeBSf_in.tBeam  NULL   MiSuBSb
/* N arm: NI input (do not get back the beam going to NE since misaligned) */
OPnode nodeNIb_in  0  nodeBSb_in.tBeam  NULL   MiSuNIb
OPnode nodeNIf_in  0  nodeNIb_in.tBeam  NULL   MiSuNIf
OPnode nodeNIb_out 0  nodeNIf_in.rBeam  NULL   MiSuNIb
OPnode nodeBSb_out 0  nodeNIb_out.tBeam NULL   MiSuBSb

/* BS output */
OPnode nodeBSf_out 0 nodeWIb_out.tBeam nodeBSb_out.tBeam  MiSuBSf

/* ********************************************************************** */
/* ------------------- Power sensing simulation -------------------------*/
/* ********************************************************************** */
/* Pick-up part of the beam to be read as B1p:
   - pick-off towards B1p: R=0.0034
   - pick-off towards phase camera 90% (this is then accounted for with a gain 1.1 in PrITF)
   - beam-splitter between d1 and d2: R=0.50  (this is then accounted for with a gain of 2 in PrITF)
   - gain of electronics (Ohm)
   - Pd quantum efficiency 90%
*/
/* MIrror name clock suspPos  thermPos   fSurf bSurf     x y z     tx ty tz */
MIrror   MirPickoff 1 NULL     NULL      NULL MiSuPickoff 0. -6. 0.  0  1  0
/* Misurf name  1/curvature radius thetax thetay halfthickness reflection losses (in intensity) */
MIsurf    MiSuPickoff  0.       .2   0.     0.     0.            0.00153     0.
/*OPnode name clock iBeam1 iBeam2 MiSurf.   output reflected beam is Pickoff.rBeam */
OPnode nodePickoff 0 nodeBSf_out.tBeam NULL   MiSuPickoff

/* B1p readout: light detection on two photodiodes d1 and d2. Gains taken from ITF procedures/DET web page*/
USignal phiDemod      -0.506  /*   30 degres */
OPdiode    d1p  0     0.90   6.2642e6  phiDemod  nodePickoff.rBeam  YES
OPdiode    d2p  0     0.90   6.2642e6  phiDemod  nodePickoff.rBeam  YES

/*
OPdet name clock efficiency demodFreq demodSignal beam shotNoise? nPd noiseAC noiseDC gainAC gainDC shaping? fAA Vmax nBits */
/* noise must be given in A/sqrtHz. ADCs have noise of 2e-7 V/sqrtHz. *
   We assume that the pre-amplifier stage has the same noise level.
   Divided by the channel gain, it gives the noise in A/sqrtHz. */
/* Pd pre-ampli gains  (V/A) from ITF procedure page:  d1pAC=35310, d1pDC=6800,    d2pAC=9520, d2pDC=390   (V/A)*/
/* A priori, the AC gains have been reduced by a factor 4 at some point (at least for d2 in June 2009 (logbook 23109) */
/*    estimated from the gains in PrITF -> d1pAC=10857,  d1pAC=1872
/* pre-ampli in ADC channels reduces the input voltage by a factor ~4.
   Then the ADC AD7674 digitizes the data with +/- 5 V input */
/*
OPdet d1p  0  0.90 6.2642e6 phiDemod  nodePickoff.rBeam  NO 1  3.7e-11  5.9e-11  10857. 6800.  NO   7.3e3  5.
18
OPdet d2p  0  0.90 6.2642e6 phiDemod  nodePickoff.rBeam  NO 1  2.1e-11  1.0e-9    1872.  390.  NO   7.3e3  5.
18
*/

/* demodulated detection photodiode signals *
(and correct for 50% splitter and 10% pickoff to phase camera, as in Virgo+ PrITF) */
USadder B1p_d1_DC_20  0 1 d1p.dc      2.2
USadder B1p_d1_ACp_20 0 1 d1p.phase   2.2
USadder B1p_d1_ACq_20 0 1 d1p.quad    2.2
USadder B1p_d2_DC_20  0 1 d2p.dc      2.2
USadder B1p_d2_ACp_20 0 1 d2p.phase   2.2
USadder B1p_d2_ACq_20 0 1 d2p.quad    2.2

UFrLRdout 1 "Pr_B1p_d1_DC"   B1p_d1_DC_20.out   1.0 -64 adc
UFrLRdout 1 "Pr_B1p_d2_ACp"  B1p_d2_ACp_20.out  1.0 -64 adc
UFrLRdout 1 "Pr_B1p_d2_ACq"  B1p_d2_ACq_20.out  1.0 -64 adc

/* Force applied to the mirror */
UFrLRdout 0 "Sc_BS_zForce"   fBS.out  1.0 -1 adc

/* True deltaL */
USignal sqrt2 1.41421356237309515
USmultiply zBSeff 1 MirBS.dxyzt.s2 sqrt2
USadder LengthN   1 2 MirNI.dxyzt.s2 zBSeff.out
                      1.0            -1.0
USadder LengthW   1 1 MirWE.dxyzt.s2 1.0
USadder deltaL    1 2 LengthN.out  LengthW.out
                      1.0           -1.0
UFrLRdout 1 "deltaL"  deltaL.out  1.0 -64 adc

/* Some channels to monitor the power at different position */
/* OPdiode name clock efficiency frequency  demodulationPhase beam shot_noise?  */
OPdiode Beam_Input       0 1 6.2642e6 NULL mod.oBeam          NO
OPdiode Beam_PRtoBS      0 1 6.2642e6 NULL nodePRf.tBeam      NO
OPdiode Beam_BStoNI      0 1 6.2642e6 NULL nodeBSb_in.tBeam   NO
OPdiode Beam_NItoBS      0 1 6.2642e6 NULL nodeNIb_out.tBeam  NO
```

```
OPdiode Beam_BStoWI        0 1 6.2642e6 NULL nodeBSf_in.rBeam  NO
OPdiode Beam_WItoWE        0 1 6.2642e6 NULL nodeWIf_in.tBeam  NO
OPdiode Beam_WEtoWI        0 1 6.2642e6 NULL nodeWEf.rBeam     NO
OPdiode Beam_WItoBS        0 1 6.2642e6 NULL nodeWIb_out.tBeam NO
OPdiode Beam_Output        0 1 6.2642e6 NULL nodeBSf_out.tBeam NO
OPdiode Beam_Pickoff       0 1 6.2642e6 NULL nodePickoff.rBeam NO
USaverage Sc_IB_TraMC_10  1 Beam_Input.dc  2
UFrLRdout 1 "Sc_IB_TraMC"      Sc_IB_TraMC_10.out  1.0 -64 adc

UFrLRdout 0 "Beam_Input"        Beam_Input.dc       1.0 -64 adc
UFrLRdout 0 "Beam_PRtoBS"       Beam_PRtoBS.dc      1.0 -1 adc
UFrLRdout 0 "Beam_BStoNI"       Beam_BStoNI.dc      1.0 -1 adc
UFrLRdout 0 "Beam_BStoWI"       Beam_BStoWI.dc      1.0 -1 adc
UFrLRdout 0 "Beam_NItoBS"       Beam_NItoBS.dc      1.0 -1 adc
UFrLRdout 0 "Beam_WItoWE"       Beam_WItoWE.dc      1.0 -1 adc
UFrLRdout 0 "Beam_WEtoWI"       Beam_WEtoWI.dc      1.0 -1 adc
UFrLRdout 0 "Beam_WItoBS"       Beam_WItoBS.dc      1.0 -1 adc
UFrLRdout 0 "Beam_Output"       Beam_Output.dc      1.0 -1 adc

UFrOFile -3 "FM_WENI"    NO FBuilder.frameH 100
```

E Siesta configuration file of AdV (WE-NI)

```
/* Simulate 130 s for suspension "warm-up" and 70 s of data usable for reconstruction */
/* maximum clock rate for OPglobal : 100 kHz */
UJclock masterClocks 4000000 4    20000. 10000. 1000.  1.
/*UFrBuilder name clock firstrun firstframe triggerType */
UFrBuilder FBuilder 3 1 1  1

/* Seismic noise */
/* Noise motion description: clock   amplitude   F_lowpass  correlation_distance*/
GRound 2     5e-7  0.6  0.
/* Noise motion at one point */
GRoundPt Mbs   0.       0.       0.
GRoundPt Mwe   0.       3005.6  0.
GRoundPt Mni   5.8      0.       0.
/*GRoundPt Mne  3005.7 0.       0.
  GRoundPt Mwi   0.       5.6      0. */

/*Simulate an initial excitation of the mirrors: sine at 0.2 Hz with linear decrase of amplitude during 0.5 s */
  USignal BSexcFreq  0.317                                              /* Hz */
  USsweep BSexcAmplTmp 0  2e-6 -2e-6                                    /* Linear variation */
  USline  BSexcTmp      0  BSexcAmplTmp.out BSexcFreq 0.0                /* Generate sine signal with decreasing amplitude */
  USif    BSexc         0  BSexcAmplTmp.out > 0 BSexcTmp.out NULL        /* Use sine signal only when amplitude is positive */
/* Force to be applied on BS mirror.  2.2V on zCorr, with 1.1 mN/V/coil -> 2.4 mN applied on each magnet */
UScosine        BSline1   0    2.2          37.0       0
UScosine        BSline2   0    2.2         117.0       0
UScosine        BSline3   0    2.2         237.0       0
USadder zBS 0 4 BSline1.out  BSline2.out  BSline3.out  BSexc.out
              0            0           0            0.0
/* Simulation of actuation  */
/*MIact name clock input f_AA(Hz) nBits DACmax(V) DACnoise(V/rHz)  gain Vmax  Imax    Rcoil  Fcoil  alpha(N/A) */
/* Since in HP mode, there is a transconductance ampli, the gain is 0.15 A/V, so we assumed Rcoil=1 and Fcoil is very high,
   being the cut-off frequency of the amplifier */
MIact    fBS 0 zBS.out     3e3       20     10.        2.5e-6            0.15 20.   1.0      1       9e3    10.6e-3

/* Force to be applied on WE mirror. 0.2 V on zCorr, with 2.2 mN/V/coil -> 0.44 mN applied on each magnet */
UScosine        WEline1   0    0.2          451.5      0
UScosine        WEline2   0    0.2          616.5      0
UScosine        WEline3   0    0.2          851.5      0
USadder zWE_UD 0 3 WEline1.out WEline2.out WEline3.out
                0            0            0
MIact    fWE_UD 0 zWE_UD.out    3e3    20   10.    2.5e-6     0.15      20.   1.0    1    9e3    1.9e-3

UScosine        WEline4   0    0.3          36.5      0
UScosine        WEline5   0    0.2        1036.5      0
USadder zWE_LR 0 2 WEline4.out WEline5.out
                0            0
MIact    fWE_LR 0 zWE_LR.out    3e3    20   10.    2.5e-6     0.15      20.   1.0    1    9e3    1.9e-3

/* ******************************************************************* */
/* -------------- Definition of the suspension and mirrors ----------------*/
/* ******************************************************************* */

/* ******* BS ****** */
Thermal     ThBS  1 5  28  15      4e6    16e6     36e6
                       0.6 4.7e3  300    600      900
                       1e6 1e6     1e5    1e5      1e5
MIsa SuBS 1 Mbs.dxyzt    "/users/rolland/home/myDev/Cali/v0r3p16/siesta/bs_tuned.sad"
                         4
                         ref_1 fBS.out
                         ref_2 fBS.out
                         ref_3 fBS.out
                         ref_4 fBS.out
                         0
                         "freeze(x,y,ty,tz)"
                        /* "defaults" */
/* Definition of the mirror  */
/* MIrror name clock suspPos  thermPos   fSurf bSurf  x y z tx  ty  tz */
MIrror    MirBS 0 SuBS.dxyzt NULL MiSuBSf MiSuBSb 0.0   0.0   0.0  -0.7 0.7 0.
/* Misurf name  1/curvature radius thetax thetay halfthickness reflection losses (in intensity) */
MIsurf    MiSuBSf 0.         .2      0.      0.      0.0         0.50       0.0e-6
MIsurf    MiSuBSb 0.         .2      0.      0.      0.0         0.00       0.0e-6

/* ******* WE ****** */
Thermal  ThWE 1 1 28
                  0.5955
                  1.e6
MIsa SuWE 1 Mwe.dxyzt    "/users/rolland/home/myDev/Cali/v0r3p16/siesta/Tower6000.sad"
                         4
                         ref_1 fWE_LR.out   /* Coil R */
                         ref_2 fWE_LR.out   /* Coil L */
                         ref_3 fWE_UD.out   /* Coil U */
```

```
                          ref_4 fWE_UD.out   /* Coil D */
                          0
                          "freeze(x,y,ty,tz)"
/* Pos of WE: (-3005.6 ;0),
     (minus half-thickness of BS at 45deg 0.5*0.065*sqrt(2) and plus WI thickness 0.2) * glass index( 1.45) */
MIrror       MirWE 1 SuWE.dxyzt  NULL MiSuWEf NULL    0. 3005.586 0.    0. -1. 0.
MIsurf       MiSuWEf  5.9417706e-4 .2 0.   0.   0.    0.999999 0

/* ******* NI ****** */
Thermal  ThNI 1 1 28
                0.5955
                1.e6
MIsa SuNI 1 Mni.dxyzt    "/users/rolland/home/myDev/Cali/v0r3p16/siesta/Tower6000.sad"
                          0
                          0
                          "freeze(x,y,ty,tz)"
/*  Pos of NI: (5.774 ; 0),
      (plus thickness of BS at 45deg 0.065*sqrt(2) and NI thickness 0.2) * glass index (1.45) */
MIrror    MirNI 1 SuNI.dxyzt  NULL MiSuNIf MiSuNIb    6.041 0. 0.    1. 0. 0.
MIsurf    MiSuNIf  7.0422535e-4  .2   0.   0.   0.    0.986   0
MIsurf    MiSuNIb  0              .2   0.   0.   0.    0.      204e-6

/* ******* NE ****** */
MIrror       MirNE 1 NULL  NULL MiSuWEf NULL    3005.841 0.   0.    -1. 0. 0.
MIsurf       MiSuNEf  5.9417706e-4 .2 0.   0.   0.    0.999999 0

/* ******* WI ******** */
MIrror    MirWI 1 NULL  NULL MiSuWIf MiSuWIb    0. 5.786 0.     0. 1. 0.
MIsurf    MiSuWIf  7.0422535e-4  .2   0.   0.   0.    0.986   0
MIsurf    MiSuWIb  0              .2   0.   0.   0.    0.      204e-6

/* ******* PR ****** */
MIrror    MirPR 1 NULL NULL MiSuPRf NULL -6.085 0. 0. 1. 0. 0.
MIsurf    MiSuPRf 6.99154e-4 .2   0. 0. 0. 0.95  530e-6     /* AdV, HR face, Roc 1430.3 m: 95% HR reflection,
                                                             <100 ppm AR reflection, <30 ppm absorption,
                                                             <400 ppm reflection in POP  of PR set in losses since misaligned */

/* ******* SR ****** */
MIrror    MirSR 1 NULL NULL MiSuSRf NULL    0.  -6.044 0.    0. 1. 0.
/*MIsurf    MiSuSRf 6.99154e-4 .2   0. 0. 0. 0. 0.000230 */      /* AdV_PR (SR with AR only) */
MIsurf    MiSuSRf 6.99154e-4 .2   0. 0. 0. 0.80 0.000130          /* AdV_SR (SR with HR) */

/* ************************************************************************ */
/* -----------------------  Laser simulation  ------------------------------*/
/* ************************************************************************ */
/*Input laser beam */
/* IOlaser  name clock surface lambda   power  powerNoise freqNoise  curvature   waist   window grid order */
IOlaser     laser 0       NULL     1064e-9  125.    NULL  NULL          0.             0.049060 0     NO   1
/*IOlaser   laser 0       NULL     1064e-9  25.     NULL  NULL      -8.8879408e-6      0.049060 0     NO   1 */

/*Modulation: OPmod name clock input nfreq  list_of_freq  signals_for_amplitude_modulation */
OPmod     mod   0  laser.oBeam  3  0. 6.270777e6 -6.270777e6 carrier NULL sb1 NULL sb2 NULL
/* Bessel J0 and J1 factors for modulation depth of 0.1 */
USignal carrier  0.997501565
USignal sb1      0.049937526
USignal sb2     -0.049937526

/* ************************************************************************ */
/* --------------------  Light propagation  ---------------------------*/
/* ************************************************************************ */
/* PR transmission of INJ beam */
OPnode nodePRf 0       mod.oBeam          NULL    MiSuPRf
/* BS front */
OPnode nodeBSf_in   0  nodePRf.tBeam      NULL    MiSuBSf

/* W arm: WI input */
OPnode nodeWIb_in   0  nodeBSf_in.rBeam  NULL    MiSuWIb
OPnode nodeWIf_in   0  nodeWIb_in.tBeam  NULL    MiSuWIf
/* W arm: WE */
OPnode nodeWEf      0  nodeWIf_in.tBeam  NULL    MiSuWEf
/* W arm: WI output */
OPnode nodeWIf_out 0  nodeWEf.rBeam      NULL    MiSuWIf
OPnode nodeWIb_out 0  nodeWIf_out.tBeam NULL    MiSuWIb

/* N arm: BS back */
OPnode nodeBSb_in   0  nodeBSf_in.tBeam  NULL    MiSuBSb
/* N arm: NI input (do not get back the beam going to NE since misaligned) */
OPnode nodeNIb_in   0  nodeBSb_in.tBeam  NULL    MiSuNIb
OPnode nodeNIf_in   0  nodeNIb_in.tBeam  NULL    MiSuNIf
OPnode nodeNIb_out 0  nodeNIf_in.rBeam  NULL    MiSuNIb
OPnode nodeBSb_out 0  nodeNIb_out.tBeam NULL    MiSuBSb

/* BS output */
OPnode nodeBSf_out 0 nodeWIb_out.tBeam nodeBSb_out.tBeam  MiSuBSf
```

```
/* SR transmission */
OPnode nodeSR 0  nodeBSf_out.tBeam      NULL  MiSuSRf

/* ********************************************************************** */
/* -------------------  Power sensing simulation  -------------------------*/
/* ********************************************************************** */
/* Pick-up part of the beam to be read as B1p:
   - pick-off towards B1p: R=0.003   (TDR, p. 299)
   - beam-splitter between d1 and d2: R=0.50
   - gain of electronics: ??,  noise of electronics: ??  (see also note VIR-0177A-12 + talk VIR-0306A-12, slide 12)
*/
/* MIrror name clock suspPos  thermPos   fSurf bSurf     x y z     tx ty tz */
MIrror   MirPickoff 1 NULL     NULL      NULL MiSuPickoff 0. -6. 0. 0  1  0
/* Misurf name  1/curvature radius thetax thetay halfthickness reflection losses (in intensity) */
MIsurf     MiSuPickoff  0.        .2   0.     0.          0.00300     0.
/*OPnode name clock iBeam1 iBeam2 MiSurf.   output reflected beam is Pickoff.rBeam */
OPnode nodePickoff 0 nodeSR.tBeam NULL   MiSuPickoff

/* B1p readout: light detection on two photodiodes d1 and d2. Gains taken from ITF procedures/DET web page*/
USignal phiDemod   -0.785398  /*   45 degres for PR_25W and PR_125W */
OPdiode    d1p  0     0.90   6.270777e6  phiDemod  nodePickoff.rBeam  YES
OPdiode    d2p  0     0.90   6.270777e6  phiDemod  nodePickoff.rBeam  YES

/* demodulated detection photodiode signals */
USadder B1p_d1_DC_20  0 1 d1p.dc     1
USadder B1p_d1_ACp_20 0 1 d1p.phase  1
USadder B1p_d1_ACq_20 0 1 d1p.quad   1
USadder B1p_d2_DC_20  0 1 d2p.dc     1
USadder B1p_d2_ACp_20 0 1 d2p.phase  1
USadder B1p_d2_ACq_20 0 1 d2p.quad   1

UFrLRdout 1 "Pr_B1p_d1_DC"   B1p_d1_DC_20.out   1.0 -64 adc
UFrLRdout 1 "Pr_B1p_d2_ACp"  B1p_d2_ACp_20.out  1.0 -64 adc
UFrLRdout 1 "Pr_B1p_d2_ACq"  B1p_d2_ACq_20.out  1.0 -64 adc

/* Force applied to the mirror */
UFrLRdout 0 "Sc_BS_zForce"   fBS.out  1.0 -1 adc

/* True deltaL */
USignal sqrt2 1.41421356237309515
USmultiply zBSeff 1 MirBS.dxyzt.s2 sqrt2
USadder LengthN   1 2 MirNI.dxyzt.s2 zBSeff.out
                      1.0            -1.0
USadder LengthW   1 1 MirWE.dxyzt.s2 1.0
USadder deltaL    1 2 LengthN.out  LengthW.out
                      1.0          -1.0
UFrLRdout 1 "deltaL"  deltaL.out  1.0 -64 adc

/* Some channels to monitor the power at different position */
/* OPdiode name clock efficiency frequency  demodulationPhase beam shot_noise?  */
OPdiode Beam_Input      0 1 6.270777e6 NULL mod.oBeam      NO
OPdiode Beam_PRtoBS     0 1 6.270777e6 NULL nodePRf.tBeam NO
OPdiode Beam_BStoNI       0 1 6.270777e6 NULL nodeBSb_in.tBeam  NO
OPdiode Beam_NItoBS       0 1 6.270777e6 NULL nodeNIb_out.tBeam NO
OPdiode Beam_BStoWI       0 1 6.270777e6 NULL nodeBSf_in.rBeam  NO
OPdiode Beam_WItoWE       0 1 6.270777e6 NULL nodeWIf_in.tBeam  NO
OPdiode Beam_WEtoWI       0 1 6.270777e6 NULL nodeWEf.rBeam     NO
OPdiode Beam_WItoBS       0 1 6.270777e6 NULL nodeWIb_out.tBeam NO
OPdiode Beam_BStoSR       0 1 6.270777e6 NULL nodeBSf_out.tBeam NO
OPdiode Beam_Output       0 1 6.270777e6 NULL nodeSR.tBeam        NO
OPdiode Beam_Pickoff      0 1 6.270777e6 NULL nodePickoff.rBeam  NO
USaverage Sc_IB_TraMC_10  1 Beam_Input.dc  2
UFrLRdout 1 "Sc_IB_TraMC"       Sc_IB_TraMC_10.out  1.0 -64 adc

UFrLRdout 0 "Beam_Input"        Beam_Input.dc       1.0 -64 adc
UFrLRdout 0 "Beam_PRtoBS"       Beam_PRtoBS.dc      1.0 -1 adc
UFrLRdout 0 "Beam_BStoNI"       Beam_BStoNI.dc      1.0 -1 adc
UFrLRdout 0 "Beam_BStoWI"       Beam_BStoWI.dc      1.0 -1 adc
UFrLRdout 0 "Beam_NItoBS"       Beam_NItoBS.dc      1.0 -1 adc
UFrLRdout 0 "Beam_WItoWE"       Beam_WItoWE.dc      1.0 -1 adc
UFrLRdout 0 "Beam_WEtoWI"       Beam_WEtoWI.dc      1.0 -1 adc
UFrLRdout 0 "Beam_WItoBS"       Beam_WItoBS.dc      1.0 -1 adc
UFrLRdout 0 "Beam_BStoSR"       Beam_BStoSR.dc      1.0 -1 adc
UFrLRdout 0 "Beam_Output"       Beam_Output.dc      1.0 -1 adc

UFrOFile -3 "FM_WENI"   NO FBuilder.frameH 100
```

F B1p readout

F.1 B1p readout in Pr

The Pr_ITF configuration files have been stored in the Virgo database and are readable through the dbui tool. The calibration parameters of B1p during the runs have been checked and are given in this appendix.

Part of the VSR4 configuration of Pr_ITF that computes the power B1p signals (20/08/2011) (the offset is given in ADC counts and the gain in W/V):

```
KEY       Name         Input          Offset  Gain     Unit  # F_Hz  DataType  ADC_gain(V/adc count)
----------------------------------------------------------------------------------------------
PR_ADC_CH B1p_d1_ACp   Pr_B1p_d1_ACp  140000 -0.000119 Watt  # 20000 32       -9.58107e-06
PR_ADC_CH B1p_d1_ACq   Pr_B1p_d1_ACq  303.86 -0.000119 Watt  # 20000 32       -9.5942e-06
PR_ADC_CH B1p_d1_DC    Pr_B1p_d1_DC   373.667 0.000167 Watt  # 20000 32       -9.58012e-06
PR_ADC_CH B1p_d1_DC_V  Pr_B1p_d1_DC   373.667 1        Volt  # 20000 32       -9.58012e-06
PR_ADC_CH B1p_d2_ACp   Pr_B1p_d2_ACp  25000  -0.000687 Watt  # 20000 32       -9.5863e-06
PR_ADC_CH B1p_d2_ACq   Pr_B1p_d2_ACq  0      -0.00069  Watt  # 20000 32       -9.56625e-06
PR_ADC_CH B1p_d2_DC    Pr_B1p_d2_DC   1175.27 0.00276  Watt  # 20000 32       -9.57021e-06
```

Part of the VSR3 configuration of Pr_ITF that computes the power B1p signals (29/08/2012), including the choice of the photodiode to use for the final channels Pr_B1p_DC, ACp, ACq:

```
KEY       Name         Input          Offset    Gain     Unit  # F_Hz  DataType ADC_gain(V/adc count)
----------------------------------------------------------------------------------------------
PR_ADC_CH B1p_d1_ACp   Pr_B1p_d1_ACp  -905.344 -0.000119 Watt  # 20000 32      -9.58107e-06
PR_ADC_CH B1p_d1_ACq   Pr_B1p_d1_ACq  303.86   -0.000119 Watt  # 20000 32      -9.5942e-06
PR_ADC_CH B1p_d1_DC    Pr_B1p_d1_DC   373.667   0.000167 Watt  # 20000 32      -9.58012e-06
PR_ADC_CH B1p_d1_DC_V  Pr_B1p_d1_DC   373.667   1        Volt  # 20000 32      -9.58012e-06
PR_ADC_CH B1p_d2_ACp   Pr_B1p_d2_ACp  846.109  -0.000687 Watt  # 20000 32      -9.5863e-06
PR_ADC_CH B1p_d2_ACq   Pr_B1p_d2_ACq  0        -0.00069  Watt  # 20000 32      -9.56625e-06
PR_ADC_CH B1p_d2_DC    Pr_B1p_d2_DC   1175.27   0.00276  Watt  # 20000 32      -9.57021e-06

# nameOut - weigth, nameIn - weigth, nameIn - ... # Unit - sample Freq
PR_SUM B1p_h_DC        2 B1p_d1_DC       # Watt 20000
PR_SUM B1p_l_DC        2 B1p_d2_DC       # Watt 20000
PR_SUM B1p_h_ACp       2 B1p_d1_ACp      # Watt 20000
PR_SUM B1p_l_ACp       2 B1p_d2_ACp      # Watt 20000
PR_SUM B1p_h_ACq       2 B1p_d1_ACq      # Watt 20000

PR_SUM B1p_l_ACq       2 B1p_d2_ACq      # Watt 20000
# nameOut - Time01 - Time10 - TrgCh - Trg01 - Trg10 - sample Freq - cmTrans # Unit
PR_TWEIGHT SW_B1p_AC       1 1 ''              0 0 20000 0 # Hit
PR_TWEIGHT SW_B1p_DC       0.0005 0.0005 B1p_d1_DC_V     8 7 20000 -2 # Hit

# nameOut - SwName - Name1 - Name2 # sample Freq - Unit
PR_SWITCH B1p_ACp_20      SW_B1p_AC       B1p_h_ACp       B1p_l_ACp       # 20000 Watt
PR_SWITCH B1p_ACq_20      SW_B1p_AC       B1p_h_ACq       B1p_l_ACq       # 20000 Watt
PR_SWITCH B1p_DC_20       SW_B1p_DC       B1p_h_DC        B1p_l_DC        # 20000 Watt

# nameOut - nameIn - Filter Type - sample Freq # Unit
PR_DECIMATE B1p_ACp         B1p_ACp_20      average    10000  # Watt
PR_DECIMATE B1p_ACq         B1p_ACq_20      average    10000  # Watt
PR_DECIMATE B1p_DC          B1p_DC_20       average    10000  # Watt
```

Part of the VSR2 configuration of Pr_ITF that computes the power B1p signals (11/12/2009):

```
KEY       Name         Input          Offset    Gain     Unit  # F_Hz  DataType ADC_gain(V/adc count)
----------------------------------------------------------------------------------------------
PR_ADC_CH B1p_d1_ACp   Pr_B1p_d1_ACp  748.23   -0.000119 Watt  # 20000 32      -9.58749e-06
PR_ADC_CH B1p_d1_ACq   Pr_B1p_d1_ACq  329.489  -0.000119 Watt  # 20000 32      -9.6168e-06
PR_ADC_CH B1p_d1_DC    Pr_B1p_d1_DC   1410.94   0.00021  Watt  # 20000 32      -9.59372e-06
PR_ADC_CH B1p_d1_DC_V  Pr_B1p_d1_DC   1410.94   1        Volt  # 20000 32      -9.59372e-06
PR_ADC_CH B1p_d2_ACp   Pr_B1p_d2_ACp  -220.411 -0.000687 Watt  # 20000 32      -9.6033e-06
PR_ADC_CH B1p_d2_ACq   Pr_B1p_d2_ACq  602.498  -0.00069  Watt  # 20000 32      -9.58876e-06
PR_ADC_CH B1p_d2_DC    Pr_B1p_d2_DC   1360.53   0.00363  Watt  # 20000 32      -9.58127e-06
```

F.2 History of B1p readout

The photodiodes deliver a current proportionnal to the beam power. The conversion factor is given in [5]: 0.78 A/W.

The equivalent resistance of the pre-amplifiers are also given: they are respectively 329 Ω and 339 Ω for the d1 and d2 photodiodes [5].

The demodulation board is described in [5]. In theory, the input gain G_1 can be changed using jumpers (defaults values are 1.7 (standard), 4 and 8), the gain of the mixer is $G_m = 0.55$ and the output gain G_2 is set to 11. It would results in a standard gain of 10.3 but it has been measured to 6.2.

The resistances giving the gain G_1 can be modified. Some history of the gains G_1 used and modified in Virgo can be found in the logbook [8].

In the demodulation board 26 used to read the d1 signal, the possible values of G_1 are 10, 30 and 100. The value[9] used since June 2009 must be 10.

In the demodulation board 29 used to read the d2 signal, the possible values of G_1 are 1.7, 4 and 8, and the value used since June 2009 is 1.7.

As a consequence, the total gain of the d1 readout is

$$G_{d1} = 0.78 \times 329 \times \left(\frac{10}{1.7} 6.2\right) = 0.78 \times 329 \times 36 \text{ W/V}$$

Taking into account the 10% increase of gain the the Pr_ITF configuration due to the phase camera pick-off, It is in agreement with the gain used Pr_ITF (0.000119): $1/G_{d1} \times 1.1 = 0.000118$.

The total gain of the d2 readout is

$$G_{d2} = 0.78 \times 339 \times 6.2 \text{ W/V}$$

Taking into account the 10% increase of gain the the Pr_ITF configuration due to the phase camera pick-off, It is in agreement with the gain used Pr_ITF (0.000690): $1/G_{d2} \times 1.1 = 0.000671$.

[8] Entries 6318, 6428, 10802 and 23109.

[9] This value of G_1 might have been used already before looking at the configuration of Pr_ITF (the gains of B1p_d2_AC were not changed between October 2008 and end 2011) but the change of G_1 from 30 to 10 between October 2005 and June 2009 (or Oct 2008) was not found in the logbook. Another possibility is that the power calibration of B1p_d1_AC was off by a factor 3 between October 2005 and June 2009.